Anharmonic order-parameter oscillations and lattice coupling in strongly driven 1 T-TaS_2 and $TbTe_3$ charge-density-wave compounds: A multiple-pulse femtosecond laser spectroscopy study

P. Kusar,[1] T. Mertelj,[1] V. V. Kabanov,[1] J.-H. Chu,[2] I. R. Fisher,[2] H. Berger,[3] L. Forró,[3] and D. Mihailovic[1]

[1]*Complex Matter Department, Jozef Stefan Institute, SI-1000 Ljubljana, Slovenia*

[2]*Geballe Laboratory for Advanced Materials, Department of Applied Physics, Stanford University, California 94304, USA*

[3]*Physics Department, École Polytechnique Federale de Lausanne, CH-1015 Lausanne, Switzerland*

(Received 8 October 2010; published 10 January 2011)

The anharmonic response of charge-density wave (CDW) order to strong laser-pulse perturbations in 1 T-TaS_2 and $TbTe_3$ is investigated by means of multiple-pump-pulse time-resolved femtosecond optical spectroscopy. We observe remarkable anharmonic effects hitherto undetected in systems exhibiting collective charge ordering. The efficiency for additional excitation of the amplitude mode by a laser pulse becomes periodically modulated after the mode is strongly excited into a coherently oscillating state. A similar effect is observed also for some other phonons, where the cross-modulation at the amplitude-mode frequency indicates anharmonic interaction of those phonons with the amplitude mode. By analyzing the observed phenomena in the framework of time-dependent Ginzburg-Landau theory we attribute the effects to the anharmonicity of the mode potentials inherent in the broken symmetry state of the CDW systems.

DOI: 10.1103/PhysRevB.83.035104 PACS number(s): 78.47.jg, 71.45.Lr, 78.47.da

I. INTRODUCTION

Ultrashort laser pulses are a convenient tool for coherent excitation of phonons[1,2] and collective electronic-lattice modes in CDW systems.[3–6] Due to the availability of strong laser pulses the phonons can be driven far from equilibrium, exposing anharmonic effects. The high-excitation region has already been investigated with single-pump-pulse[7–10] and double-pump-pulse[8,11,12] sequences, mainly in elemental Bi, Sn, and Te.

In charge density wave (CDW) systems the phonon-mode potentials are inherently anharmonic due to their coupling to the electron density modulation.[13] The anharmonicity is the strongest for the Kohn-anomaly[14] modes, which become the amplitude and phase modes in the CDW state. While amplitude modes (AM) have been extensively investigated in near-equilibrium conditions by Raman[14,15] and time-resolved spectroscopy[3–6,16] as well as in the highly driven nonequilibrium conditions, where the CDW order is destroyed,[17–20] so far little attention has been paid to the region in between.[18]

Here we report on an investigation of a hitherto unexplored aspect of the CDW amplitude mode behavior under strongly driven nonequilibrium conditions in the ordered phase below the CDW photoinduced destruction threshold. Contrary to previous standard double-pump pulse (SDPP) high-excitation work,[8,11,12] where a pair of balanced pump pulses was used, we introduce an unbalanced double-pump-pulse (UDPP) approach in which we use the first and strongest pump pulse (P_1) to excite large-amplitude coherent oscillations of the AM and other phonon modes and then use a standard pump-probe (P_2-p_3) pulse sequence to interrogate the system. By means of this approach we are able to directly investigate the anharmonicity of the effective AM potential, as well as detect the anharmonic coupling of the collective bosonic mode (the AM) of the CDW to other lattice modes.

II. EXPERIMENTAL

To establish generality, two layered chalcogenides which show different types of CDW ordering and also different electronic properties were investigated: $TbTe_3$ and 1T-TaS_2. (Sample growth is described in Ref. 21 for $TbTe_3$ and Ref. 22 for 1T-TaS_2.) $TbTe_3$ is a two-dimensional (2D) metal which shows a unidirectional incommensurate CDW state at the temperature used in our experiment (15 K),[23,24] while 1T-TaS_2 is in a commensurate insulating CDW state at the relevant temperature (77 K).[25] In both systems, in addition to the AM, several new Raman modes appear in the CDW state due to Brillouin-zone folding.[4,6,14,26,27]

In our experiments the three pulse trains were derived from a 50-fs 250-kHz Ti:Al_2O_3 regenerative amplifier, with $\hbar\omega_P = 1.55$ eV photon energy. The p_3 polarization was perpendicular to P_1 and P_2, which were parallel to each other. To study the reflectivity change induced by the weaker P_2 pulse, $\Delta R_2(t)$, we eliminate the P_1 contribution $\Delta R_1(t)$ to the total transient reflectivity $\Delta R(t)$ by means of the homodyne detection locked to the modulation of the P_2 pulse train. [The P_1 pulse train was unmodulated, as shown in Fig. 1(b).]

III. RESULTS

In Fig. 1(a) we plot the raw UDPP photoinduced reflectivity transients $\Delta R_2(t_{23})/R$ in 1 T-TaS_2 at different delays t_{12} between the pump pulses. The intensity of the P_2 pulse train, I_2, was set in the linear response region while the intensity of the P_1 pulse train was four times larger, corresponding to ~30% of the CDW destruction threshold fluence. For comparison the raw total photoinduced reflectivity transients $\Delta R(t_{23})/R$, measured in SDPP configuration, are shown in Fig. 1(c). In both cases the amplitude of the coherent oscillations periodically varies as t_{12} is increased, with a clear periodic suppression of the oscillations. Note that the suppression appears at different t_{12} for each case. While the

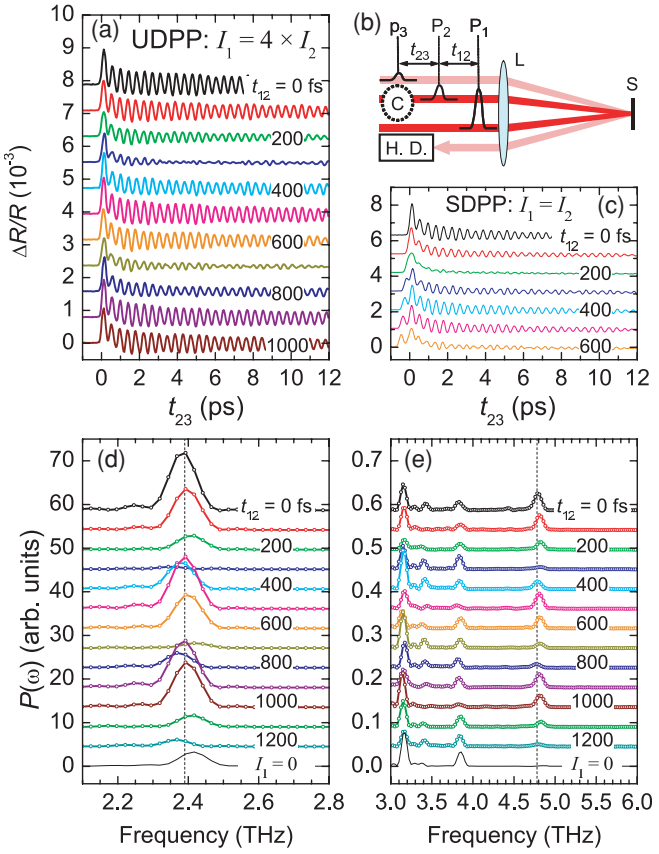

FIG. 1. (Color online) $\Delta R/R$ transients as a function of t_{12} in 1 T-TaS_2 (a) in the UDPP configuration shown in the schematics (b); L = lens, S = sample, C = chopper, H.D. = homodyne detection system. For comparison, $\Delta R/R$ transients in the SDPP configuration are shown in (c). The lower graphs show UDPP power spectra in 1 T-TaS_2 around the fundamental frequency of the strongest mode (d) and around the second harmonic of the fundamental frequency (e). The thin curve in (d) and (e) is the standard single-pump-pulse spectrum.

linear SDPP effect [Fig. 1(c)] is well known,[16,28–30] and is understood as an interference due to the linear superposition of two independently excited coherent oscillations,[16,29,30] the nonlinear effects observed by UDPP have not been detected before.

In Figs. 1(d) and 1(e) we plot the power spectra of the UDPP transients from Fig. 1(a). In addition to the AM mode with the frequency 2.41 THz we observe several weaker phonon modes above 3 THz and a weak second harmonic of the AM mode [see Fig. 1(e)]. The periodic intensity modulation of the modes, which strongly increases with increasing I_2 (see Fig. 2), is accompanied by a small periodic frequency shift. The shift is absent in the low-excitation SDPP configuration [see Figs. 2(c) and 2(f)]. The modulation amplitude and phase vary among the modes, and there is a $\sim\pi/2$ shift between the modulation phases of the UDPP and SDPP cases, similar to the observations in the high-excitation-density SDPP experiment in Te.[11] In our case however, the phase shift persists down to the lowest excitation density.

The periodic intensity modulation and the phase shift are observed also in $TbTe_3$, where in addition a beating in the

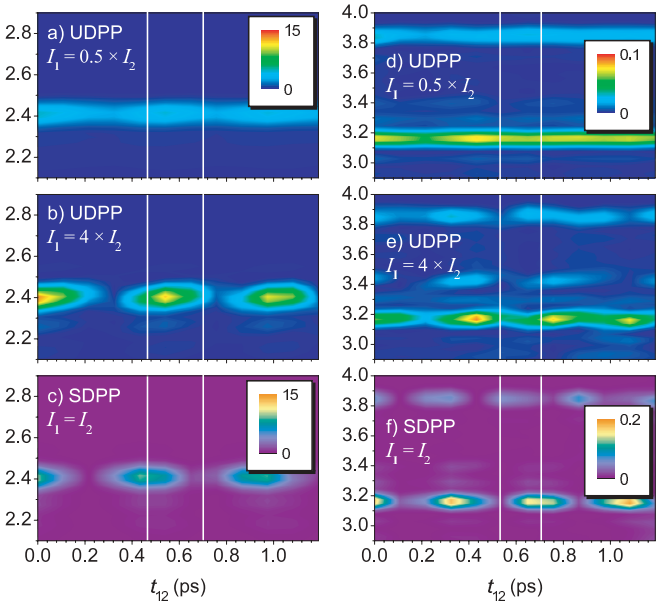

FIG. 2. (Color online) Spectra of the strongest mode (a), (b), and weaker modes (d), (e), as functions of t_{12} in the UDPP configuration at different intensities of the P_1 pulse train in 1 T-TaS_2. For comparison the low-excitation SDPP-configuration spectra are shown in (c) and (f).

t_{12} dependence of the modulation amplitudes is observed [see Fig. 3(c)].

The modulation frequency of each mode [see Figs. 3(b) and 3(d)] is correlated to the respective mode eigenfrequency. Surprisingly, in the UDPP configuration there is also a clear cross-modulation of the 3.38-THz and 3.85-THz mode intensities with the 2.41-THz AM frequency, and of the

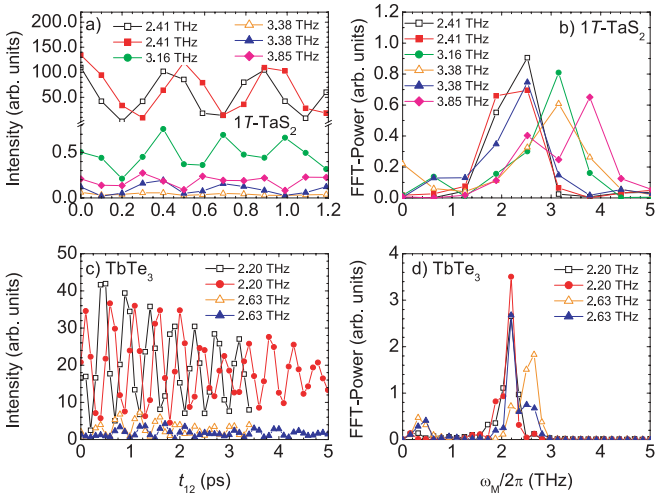

FIG. 3. (Color online) Integrated intensities of the strongest modes as functions of t_{12} in UDPP configuration (a) at $I_1 = 4 \times I_2$ in 1 T-TaS_2 and (c) at $I_1 = 2.4 \times I_2$ in $TbTe_3$. Normalized power spectra of the traces are shown in panels (b) and (d). Open symbols correspond to the low-intensity SDPP response. Note the difference in the modulation frequency for the 3.38-THz mode in 1T-TaS_2 (b) and the 2.63-THz mode in $TbTe_3$ (d) between the UDPP (full triangles) and SDPP (open triangles) cases.

2.63-THz mode intensity with the 2.20-THz AM frequency, in 1 T-TaS_2 and $TbTe_3$, respectively.

IV. DISCUSSION

To understand the observed phenomena we start with the simplest Ginzburg-Landau expansion of the free energy:

$$F = F_0 + \left(\frac{T}{T_c} - 1\right)|A|^2 + \frac{1}{2}|A|^4 + g(t)|A|^2, \qquad (1)$$

in terms of the normalized complex order parameter A. T_c is the critical temperature and $g(t)$ represents the external laser excitation. Due to the symmetry $g(t)$ can couple only to $|A|^2$. To describe the dynamics we introduce the $T = 0$ AM frequency ω_0 and the dimensionless damping $\gamma = \Delta\omega_0/\omega_0$, and obtain using Eq. (1)

$$\frac{2}{\omega_0^2}\frac{\partial^2}{\partial t^2}A + \frac{4\gamma}{\omega_0}\frac{\partial}{\partial t}A + \left(\frac{T}{T_c} - 1\right)A + |A|^2 A = -g(t)A. \qquad (2)$$

Since $g(t)A$ cannot excite phase fluctuations, only the AM needs to be considered. (In the equilibrium, A can always be set real by a proper choice of the phase.) According to Ref. 31, the dielectric constant depends in the lowest order on $|A|^2$:

$$\epsilon = \epsilon_0 + c_1|A|^2, \qquad (3)$$

so the reflectivity change in the UDPP configuration is written as

$$\Delta R_2(t) = \Delta R(t) - \Delta R_1(t) \propto |A(t)|^2 - |A_1(t)|^2, \qquad (4)$$

where $A_1(t)$ is the solution of Eq. (2) with excitation from the P_1 pulse only and $A(t)$ is the solution with the excitation from both pump pulses.

There are two terms in Eq. (2) that are of interest: $g(t)A$ and $|A|^2A$. The term $g(t)A$ leads to a periodic modulation of the coupling of A to the P_2 pulse when the oscillation amplitude after the P_1 pulse is large. This effect, however, does not explain the main features of our observations: (i) if the oscillation amplitude is large, a significant AM-overtone intensity is expected due to $|A|^2$ in Eq. (3), which is not observed in the experiment; (ii) because the laser excitation initially drives A toward zero an intermediate amplitude of the oscillations at $t_{12} = 0$ followed by a minimum at $\omega_0 t_{12} \simeq \pi/2$, where $A(t)$ is closest to 0, is expected. (The term $g(t)$ couples to A as T so a positive $g(t)$ decreases A.) Instead, the first minimum is observed around $\omega_0 t_{12} \simeq 3\pi/2$ and the amplitude is the largest at $t_{12} = 0$ in 1 T-TaS_2 and at $\omega_0 t_{12} \simeq \pi/2$ in $TbTe_3$. The anharmonic term $|A|^2A$ in Eq. (2) remains therefore the only possible origin of the observed behavior.

The solutions of Eq. (2) with $\gamma = 0$ can be represented as closed periodic orbits in the phase space [see Fig. 4(a)]. Due to the anharmonicity, the frequency of the orbit decreases with the oscillation amplitude. The P_2 pulse transfers the system from the initial orbit, set by the P_1 pulse, to a final orbit with a different frequency, which depends on t_{12}. This results in a beating of the $\Delta R_2(t)$ oscillations due to an interference of the second and the first term in the right-hand side of Eq. (4), corresponding to the initial and final orbits, respectively. The frequency of the final orbit periodically oscillates with increasing t_{12} [see Fig. 4(b)]. Within a single initial orbit period there exist two delays, $\omega_0 t_{12} \sim \phi_0 + \pi/2$ and $\sim \phi_0 + 3\pi/2$, at which the only effect of the P_2 pulse is a phase shift within the initial orbit. In the vicinity of these delays the beating is very slow, resulting in a slow increase of the $\Delta R_2(t)$ oscillations amplitude with t. This slow rise is suppressed when γ is finite since the oscillations die out before a significant phase shift between the orbits builds up, and the $\Delta R_2(t)$ oscillations amplitude remains small. As a result a periodic modulation of the $\Delta R_2(t)$ oscillations amplitude is observed in the simulations with finite γ [see Fig. 4(c)]. In addition to the more intensive maximum, reminiscent of the experimental observations, an additional weak maximum is observed within a single period corresponding to t_{12} with the larger final-orbit frequency [see Fig. 4(b)]. The weak maximum is strongly sensitive to the characteristic timescale of the external laser perturbation, τ_g, and is completely suppressed by setting $\tau_g = 2\pi/\omega_0$, as shown in Fig. 4(d). (In simulations $g(t) = g_1 f(t) + g_2 f(t - t_{12})$, with $f(t) = \exp(-t/\tau_g)/[1 + \exp(-10t/\tau_g)]$, was used to represent P_1 and P_2.)

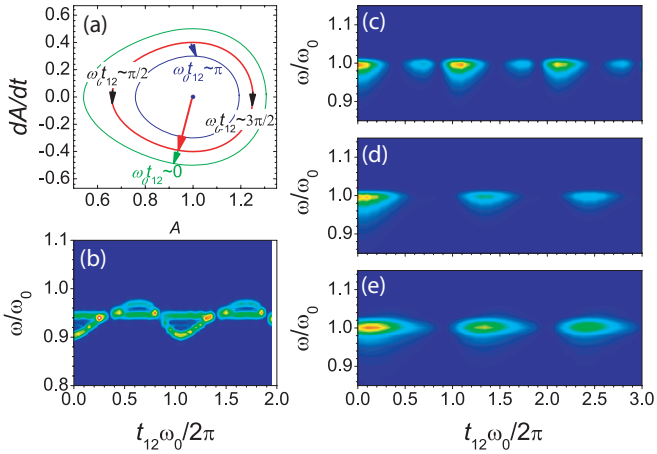

FIG. 4. (Color online) (a) Orbits of Eq. (2) in the phase space in the absence of damping ($\gamma = 0$). The long arrow represents the initial excitation by the P_1 pulse. The short arrows represent the additional excitation by the P_2 pulse, which transfers the system to different orbits depending on t_{12}. Simulated power spectrum as a function of t_{12} in the absence of damping is shown in (b); with damping ($\gamma = 0.01$) and short excitation pulses, $\omega_0\tau_g = 0.2\pi$, (c); with damping and long excitation pulses $\omega_0\tau_g = 2\pi$, (d); with damping, long excitation pulses, and a finite laser penetration depth, $\lambda/\xi = 16$, (e).

To improve agreement of the model with the experiment we extended the Ginzburg-Landau expansion [Eq. (1)] with the gradient term $\xi^2|\partial A/\partial z|^2$ (see Ref. 20) to allow for space variations of the order parameter perpendicular to the sample surface due to the finite penetration depth λ of the laser pulses. The result of a simulation with the inhomogeneous order parameter [Fig. 4(e)] better reproduces the main experimental features for the AM. Similarly to the homogeneous case, the weak maximum, which is not observed in the experiment, is absent only as long as $\omega_0\tau_g \sim 2\pi$. In our experiment $\omega_0\tau_l \sim 0.2\pi$, where τ_l is the length of the laser pulses, indicating that the coherent oscillations are not excited by the impulsive stimulated-Raman-scattering mechanism,[2] but rather by the displacive one,[1] which can lead to $\tau_g > \tau_l$.

Counterintuitively, the experimentally observed small periodic frequency modulation of the AM is not reproduced in any simulation with a finite damping, so the origin of the effect is beyond the present model.

Next we turn to analysis of the weaker modes, with displacements denoted Q_i. As in the case of the AM we can exclude the direct driving terms $|Q_i|^2 g(t)$ and $\Re(Q_i A^*)g(t)$ as the sources of the modulation because of the relatively small displacements. However, in addition to the AM other modes can also be coupled to the CDW charge modulation. As a result, mode displacements Q_i become mixed with the AM displacement A, and the effective mixed-mode potentials become anharmonic. [The terms $\Re(Q_i A^*)$ must be added to the total free energy.] This leads to the cross-modulation of mode intensities with the AM frequency in addition to the self-modulation at the particular mode eigenfrequency. The relative amounts of the modulation at both frequencies depend on the couplings to the AM and to the external laser perturbation. If after the P_1 pulse the amplitude of a particular mode is small, the main contribution to the modulation is due to the cross-modulation at the AM frequency, as is the case for the 3.38-THz mode in 1 T-TaS_2 and the 2.63-THz mode in $TbTe_3$. If, on the other hand, the amplitude is large enough, a significant self-modulation is expected as in the case of the 3.85-THz mode in 1 T-TaS_2.

The observed modulation and cross-modulation can be related to the recent proposal of Schäfer *et al.*[13] for quasi-1D CDW in $K_{0.3}MoO_3$. According to Schäfer *et al.* the overdamped electronic part of the order parameter is linearly coupled to several different modes of the same symmetry in the CDW state. In $K_{0.3}MoO_3$ the three strongest Raman active modes show rather similar couplings. No distinction can be made among them and no clear lattice soft mode can be identified in this case on the basis of the linear response. The determination of the cross-modulation among different phonon modes at larger excitation levels could therefore further clarify their roles in the CDW transition. Indeed, some difference between the intensity modulation of different modes in $K_{0.3}MoO_3$ has recently been observed after the destruction of the CDW by a laser pulse.[20] We therefore believe that the determination of the cross-modulation among different modes in other CDW compounds could further clarify the roles of different phonons in CDW transitions.

V. CONCLUSIONS

In conclusion, by means of unbalanced double-pump-pulse time-resolved optical spectroscopy, we were able to detect the inherent broken-symmetry-state anharmonicity of the amplitude-mode effective potential in two distinct CDW systems. We also found clear evidence of the anharmonic mixing of certain phonon modes with the amplitude mode originating from their mutual coupling to the electronic-density CDW modulation. We showed that the observed effects can be described in the framework of time-dependent Ginzburg-Landau theory.

ACKNOWLEDGMENTS

This work has been supported by the Slovenian Research Agency and the CENN Nanocenter.

[1] H. J. Zeiger, J. Vidal, T. K. Cheng, E. P. Ippen, G. Dresselhaus, and M. S. Dresselhaus, Phys. Rev. B **45**, 768 (1992).
[2] R. Merlin, Solid State Commun. **102**, 207 (1997).
[3] J. Demsar, K. Biljakovic, and D. Mihailovic, Phys. Rev. Lett. **83**, 800 (1999).
[4] J. Demsar, L. Forró, H. Berger, and D. Mihailovic, Phys. Rev. B **66**, 041101 (2002).
[5] D. Sagar, A. Tsvetkov, D. Fausti, S. van Smaalen, and P. van Loosdrecht, J. Phys. Condens. Matter **19**, 346208 (2007).
[6] R. V. Yusupov, T. Mertelj, J.-H. Chu, I. R. Fisher, and D. Mihailovic, Phys. Rev. Lett. **101**, 246402 (2008).
[7] S. Hunsche, K. Wienecke, T. Dekorsy, and H. Kurz, Phys. Rev. Lett. **75**, 1815 (1995).
[8] M. F. DeCamp, D. A. Reis, P. H. Bucksbaum, and R. Merlin, Phys. Rev. B **64**, 092301 (2001).
[9] M. Hase, M. Kitajima, S.-i. Nakashima, and K. Mizoguchi, Phys. Rev. Lett. **88**, 067401 (2002).
[10] O. V. Misochko, M. Hase, K. Ishioka, and M. Kitajima, Phys. Rev. Lett. **92**, 197401 (2004).
[11] C. A. D. Roeser, M. Kandyla, A. Mendioroz, and E. Mazur, Phys. Rev. B **70**, 212302 (2004).
[12] E. D. Murray, D. M. Fritz, J. K. Wahlstrand, S. Fahy, and D. A. Reis, Phys. Rev. B **72**, 060301 (2005).
[13] H. Schäfer, V. V. Kabanov, M. Beyer, K. Biljakovic, and J. Demsar, Phys. Rev. Lett. **105**, 066402 (2010).
[14] S. Sugai, Phys. Status Solidi B **129**, 13 (1985).
[15] M. Lavagnini *et al.*, Phys. Rev. B **78**, 201101 (2008).
[16] T. Onozaki, Y. Toda, S. Tanda, and R. Morita, Jpn. J. Appl. Phys. **46**, 870 (2007).
[17] L. Perfetti, P. A. Loukakos, M. Lisowski, U. Bovensiepen, H. Berger, S. Biermann, P. S. Cornaglia, A. Georges, and M. Wolf, Phys. Rev. Lett. **97**, 067402 (2006).
[18] F. Schmitt *et al.*, Science **321**, 1649 (2008).
[19] A. Tomeljak, H. Schäfer, D. Städter, M. Beyer, K. Biljakovic, and J. Demsar, Phys. Rev. Lett. **102**, 066404 (2009).
[20] R. V. Yusupov, T. Mertelj, P. Kusar, V. Kabanov, S. Brazovskii, J.-H. Chu, I. R. Fisher, and D. Mihailovic, Nature Physics **6**, 681 (2010).
[21] N. Ru, J.-H. Chu, and I. R. Fisher, Phys. Rev. B **78**, 012410 (2008).
[22] B. Dardel, M. Grioni, D. Malterre, P. Weibel, Y. Baer, and F. Lévy, Phys. Rev. B **45**, 1462 (1992).
[23] E. DiMasi, M. C. Aronson, J. F. Mansfield, B. Foran, and S. Lee, Phys. Rev. B **52**, 14516 (1995).
[24] A. Fang, N. Ru, I. R. Fisher, and A. Kapitulnik, Phys. Rev. Lett. **99**, 046401 (2007).
[25] R. E. Thomson, B. Burk, A. Zettl, and J. Clarke, Phys. Rev. B **49**, 16899 (1994).

[26]T. Hirata and F. S. Ohuchi, Solid State Commun. **117**, 361 (2001).
[27]M. Lavagnini, H.-M Eiter, L. Tassini, B. Muschler, R. Hackl, R. Monnier, J.-H Chu, I. R. Fisher, and L. Degiorgi, Phys. Rev. B **81**, 081101(R) (2010).
[28]T. Dekorsky, W. Kütt, T. Pfeifer, and H. Kurz, Europhys. Lett. **23**, 223 (1993).
[29]M. Hase, K. Mizoguchi, H. Harima, S. Nakashima, M. Tani, K. Sakai, and M. Hangyo, Appl. Phys. Lett. **69**, 2474 (1996).
[30]D. Mihailovic, D. Dvorsek, V. Kabanov, J. Demsar, L. Forro, and H. Berger, Appl. Phys. Lett. **80**, 871 (2002).
[31]V. Ginzburg, A. Levanyuk, and A. Sobyanin, Phys. Rep. **57**, 151 (1980).